ELSEVIER

Spectrochimica Acta Part B 62 (2007) 1528 – 1536

SPECTROCHIMICA ACTA PART B

www.elsevier.com/locate/sab

Laser-induced breakdown spectroscopy analysis of minerals: Carbonates and silicates ☆

Nancy J. McMillan [a,*], Russell S. Harmon [b], Frank C. De Lucia [c], Andrzej M. Miziolek [c]

[a] *Department of Geological Sciences, Box 30001, MSC 3AB, New Mexico State University, Las Cruces, NM 88003, USA*
[b] *Environmental Sciences Division, US Army Research Office, Research Triangle Park, NC 27709, USA*
[c] *Weapons and Material Sciences Directorate, US Army Research Laboratory, Aberdeen Proving Ground, MD 21005, USA*

Received 8 December 2006; accepted 22 October 2007
Available online 26 November 2007

Abstract

Laser-induced breakdown spectroscopy (LIBS) provides an alternative chemical analytical technique that obviates the issues of sample preparation and sample destruction common to most laboratory-based analytical methods. This contribution explores the capability of LIBS analysis to identify carbonate and silicate minerals rapidly and accurately. Fifty-two mineral samples (18 carbonates, 9 pyroxenes and pyroxenoids, 6 amphiboles, 8 phyllosilicates, and 11 feldspars) were analyzed by LIBS. Two composite broadband spectra (averages of 10 shots each) were calculated for each sample to produce two databases each containing the composite LIBS spectra for the same 52 mineral samples. By using correlation coefficients resulting from the regression of the intensities of pairs of LIBS spectra, all 52 minerals were correctly identified in the database. If the LIBS spectra of each sample were compared to a database containing the other 51 minerals, 65% were identified as a mineral of similar composition from the same mineral family. The remaining minerals were misidentified for two reasons: 1) the mineral had high concentrations of an element not present in the database; and 2) the mineral was identified as a mineral with similar elemental composition from a different family. For instance, the Ca–Mg carbonate dolomite was misidentified as the Ca–Mg silicate diopside. This pilot study suggests that LIBS has promise in mineral identification and *in situ* analysis of minerals that record geological processes.

Keywords: Laser-induced breakdown spectroscopy; LIBS; Mineral; Carbonate; Silicate

1. Introduction

Minerals are the fundamental chemical building blocks of solid earth materials. Identification of the mineral assemblage present in a rock provides a wealth of information about the history of the rock such as the pressure, temperature, and chemical environment of its formation; the pressure and temperature conditions of any post-formation hydrothermal alteration or recrystallization events; evidence for exsolution; and the extent of weathering at the Earth's surface.

More than 3800 distinct mineral species have been identified on Earth [1]. Because correct identification of minerals and knowledge about their chemical composition is critical to an understanding of the genesis and history of any particular rock body, several methods are routinely used to identify minerals. The physical properties of minerals (hardness, color, streak, luster, direction and quality of cleavage, habit, magnetism, reaction with hydrochloric acid) are used in the field to identify minerals. To be successful, these tests require extensive knowledge and experience on the part of the investigator; even then they are not necessarily definitive. More sophisticated techniques [1,2] are required for extremely fine-grained minerals or to distinguish between minerals with similar physical properties (e.g. white minerals of the same or similar crystal habit). Most minerals are transparent to translucent in sections 30 μm thick (thin sections) and have distinct optical properties when viewed under polarized light. Again, mineral identification by polarized light depends on

☆ This paper was presented at the 4th International Conference on Laser Induced Plasma Spectroscopy and Applications (LIBS 2006) held in Montreal, Canada, 5–8 September 2006, and is published in the Special Issue of Spectrochimica Acta Part B, dedicated to that conference.

* Corresponding author. Tel.: +1 505 646 5000; fax: +1 505 646 1056.
E-mail address: nmcmilla@nmsu.edu (N.J. McMillan).

0584-8547/$ - see front matter © 2007 Elsevier B.V. All rights reserved.
doi:10.1016/j.sab.2007.10.037

Report Documentation Page

Form Approved
OMB No. 0704-0188

1. REPORT DATE	2. REPORT TYPE	3. DATES COVERED
DEC 2006		**00-00-2006 to 00-00-2006**

4. TITLE AND SUBTITLE	5a. CONTRACT NUMBER
Laser-induced breakdown spectroscopy analysis of minerals: Carbonates and silicates	5b. GRANT NUMBER
	5c. PROGRAM ELEMENT NUMBER
6. AUTHOR(S)	5d. PROJECT NUMBER
	5e. TASK NUMBER
	5f. WORK UNIT NUMBER
7. PERFORMING ORGANIZATION NAME(S) AND ADDRESS(ES) **US Army Research Office,Environmental Sciences Division,Research Triangle Park,NC,27709**	8. PERFORMING ORGANIZATION REPORT NUMBER
9. SPONSORING/MONITORING AGENCY NAME(S) AND ADDRESS(ES)	10. SPONSOR/MONITOR'S ACRONYM(S)
	11. SPONSOR/MONITOR'S REPORT NUMBER(S)

12. DISTRIBUTION/AVAILABILITY STATEMENT
Approved for public release; distribution unlimited

13. SUPPLEMENTARY NOTES

14. ABSTRACT

Laser-induced breakdown spectroscopy (LIBS) provides an alternative chemical analytical technique that obviates the issues of sample preparation and sample destruction common to most laboratory-based analytical methods. This contribution explores the capability of LIBS analysis to identify carbonate and silicate minerals rapidly and accurately. Fifty-two mineral samples (18 carbonates, 9 pyroxenes and pyroxenoids, 6 amphiboles, 8 phyllosilicates, and 11 feldspars) were analyzed by LIBS. Two composite broadband spectra (averages of 10 shots each) were calculated for each sample to produce two databases each containing the composite LIBS spectra for the same 52 mineral samples. By using correlation coefficients resulting from the regression of the intensities of pairs of LIBS spectra, all 52 minerals were correctly identified in the database. If the LIBS spectra of each sample were compared to a database containing the other 51 minerals, 65% were identified as a mineral of similar composition from the same mineral family. The remaining minerals were misidentified for two reasons: 1) the mineral had high concentrations of an element not present in the database; and 2) the mineral was identified as a mineral with similar elemental composition from a different family. For instance, the Ca?Mg carbonate dolomite was misidentified as the Ca?Mg silicate diopside. This pilot study suggests that LIBS has promise in mineral identification and in situ analysis of minerals that record geological processes.

15. SUBJECT TERMS

16. SECURITY CLASSIFICATION OF:			17. LIMITATION OF ABSTRACT	18. NUMBER OF PAGES	19a. NAME OF RESPONSIBLE PERSON
a. REPORT **unclassified**	b. ABSTRACT **unclassified**	c. THIS PAGE **unclassified**	**Same as Report (SAR)**	**9**	

Table 1
Formulas of carbonate minerals used in this study

Mineral	Formula
Hexagonal rhombohedral carbonates	
Calcite (4) [a]	$CaCO_3$
Dolomite	$CaMg(CO_3)_2$
Magnesite	$MgCO_3$
Rhodochrosite (2)	$MnCO_3$
Siderite	$FeCO_3$
Smithsonite (3) [b]	$ZnCO_3$
Orthorhombic carbonates	
Aragonite (2)	$CaCO_3$
Cerussite	$PbCO_3$
Strontianite	$SrCO_3$
Witherite	$BaCO_3$
Monoclinic carbonates	
Azurite	$Cu_3(CO_3)_2(OH)_2$

[a] Numbers in parentheses indicate the number of samples analyzed in this study. Unless specified, one sample was analyzed.
[b] Smithsonite samples included blue, green, and purple varieties.

the skill and knowledge of the microscopist. X-ray diffraction (XRD) measures the distances between planes of atoms in the crystal structure, permitting accurate identification of even very fine-grained minerals. The fine-scale chemical composition of minerals is commonly determined using electron microprobe analysis (EMPA) of polished thin sections. EMPA technology has expanded during recent years to measure trace element compositions. Major and trace element concentrations in minerals are also determined using Laser-Ablation Inductively Coupled Plasma Mass Spectrometry (LA–ICPMS). Each of these techniques provides a unique and useful data set. However, these laboratory techniques are time consuming and destructive.

Across many different areas of the geosciences, there has been a long-standing requirement for a real-time technique for in-field mineral identification and chemical analysis. The development of portable XRF and Raman spectrometry systems over the past decade has met this need to a limited degree. Broadband Laser-Induced Breakdown Spectroscopy (LIBS) has the potential to measure all elements in rocks, minerals, and soils in real-time with no sample preparation. Field-portable LIBS systems are in development [3,4].

Because field-portable LIBS is on the horizon, and because there are many potential mineralogical applications for LIBS, it is appropriate to examine the capability of this technique to identify minerals. LIBS is one of the analytical technologies planned for next generation of Mars rovers [5]; the use of standoff LIBS will expand the geographical area that can be chemically analyzed from the rover.

On Earth, many prospecting techniques rely on the identification of certain key mineral assemblages or chemical signatures in minerals as "pathfinders." For instance, kimberlitic diamonds are commonly associated with significantly more abundant Cr-diopside pyroxenes and garnets with high Cr/Ca ratios [6,7]. Many rock units exhibit spatial variations in mineral composition that provide clues to the processes that formed or recrystallized the rock. For example, Parker and Nicholson [8] used As variations in geothermal sinters (amorphous silica) as a guide to gold enrichment. Currently, these variations are mapped by collecting samples along one or more traverse(s) across the unit, followed by sample preparation and analysis in the laboratory. The mapping process could be extended to cover the entire three-dimensional exposure of the rock unit, using field-portable LIBS, if LIBS spectra are sufficiently sensitive to mineral chemistry.

This paper explores LIBS analysis of two important mineral groups: the carbonates and the silicates. Samples from the teaching collection at New Mexico State University that are representative of the natural range of composition of common carbonate and silicate minerals were analyzed by benchtop LIBS at the Army Research Laboratory (ARL). These data were used to determine whether LIBS 1) can be used to identify minerals; 2) is able to readily differentiate between members within a group of structurally similar minerals; and 3) is sensitive to mineral composition or stoichiometry.

2. Theoretical: mineral structures and compositions

2.1. Carbonates

The carbonates comprise a class of minerals in which a metal ion is coordinated by the CO_3^{2-} carbonate molecule. Carbonate mineral structures (Table 1) are either hexagonal rhombohedral,

Table 2
Formulas of silicate minerals used in this study

Mineral	Formula
Pyroxenes and pyroxenoids	
Aegirine	$NaFeSi_2O_6$
Augite	$(Ca,Na)(Mg,Fe,Al)(Si,Al)_2O_6$
Diopside (2)[a]	$CaMgSi_2O_6$
Orthopyroxene (2)	$(Mg,Fe)SiO_3$
Rhodonite	$MnSiO_3$
Spodumene	$LiAlSi_2O_6$
Wollastonite	$CaSiO_3$
Amphiboles	
Actinolite	$Ca_2(Mg,Fe)_5Si_8O_{22}(OH)_2$
Anthophyllite	$(Mg,Fe)_7Si_8O_{22}(OH)_2$
Glaucophane	$Na_2\ Mg_3Al_2Si_8O_{22}(OH)_2$
Hornblende	$(Ca,Na)_{2-3}(Mg,Fe,Al)_5Si_6(Si,Al)_2O_{22}(OH)_2$
Riebeckite	$Na_2Fe_5Si_8O_{22}(OH)_2$
Tremolite	$Ca_2\ Mg_5Si_8O_{22}(OH)_2$
Phyllosilicates	
Biotite	$K(Mg,Fe)_3AlSi_3O_{10}(OH)_2$
Lepidolite	$K(Li,Al)_{2-3}AlSi_3O_{10}(O,OH,F)_2$
Muscovite (2)	$KAl_2AlSi_3O_{10}(OH)_2$
Phlogopite	$KMg_3AlSi_3O_{10}(OH)_2$
Serpentine (2)	$Mg_6Si_4O_{10}(OH)_8$
Talc	$Mg_3Si_4O_{10}(OH)_2$
Feldspars	
K-feldspar (3)	$(K,Na)AlSi_3O_8$
Plagioclase (8)	$NaAlSi_3O_8–CaAl_2Si_2O_8$

Mineral formulas from Klein [1].
[a] Numbers in parentheses indicate the number of samples analyzed in this study. Unless specified, one sample was analyzed.

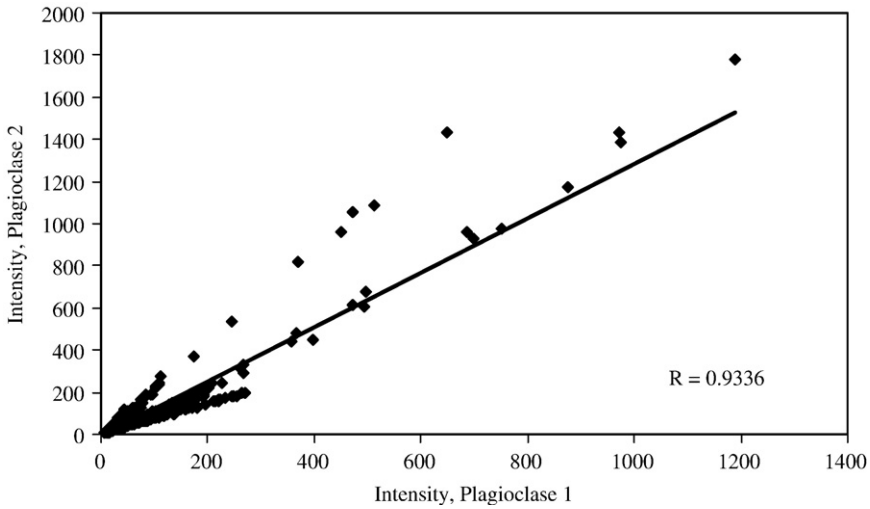

Fig. 1. Correlation of two LIBS spectra against each other. The intensity of each pixel for sample Plagioclase 1 is plotted against the intensity of the corresponding pixel for sample Plagioclase 2. The line is the result of a linear regression of the two spectra. The linear trend of data above the regression line records a peak that has higher intensity in sample Plagioclase 2 than in Plagioclase 1.

orthorhombic, or monoclinic, depending on whether the metal ion is small (rhombohedral) or large (orthorhombic), or whether the carbonate is hydrous (monoclinic). This structural flexibility and the nearly ubiquitous presence of the carbonate molecule at and near the Earth's surface result in the widespread occurrence of the carbonates in rocks formed by sedimentary, hydrothermal, metamorphic, and weathering processes.

2.2. Silicates

Known as the "rock-forming" minerals, silicates are the dominant minerals in the Earth's crust and mantle. Three groups of silicates are considered in this paper: the inosilicates, phyllosilicates, and feldpsars (Table 2). The inosilicates (pyroxenes, pyroxenoids, and amphiboles) have chains of silica tetrahedra parallel to the *c*-crystallographic axis. The phyllosilicates, or layer silicates, are composed of alternating sheets of tetrahedra and sheets of octahedra. The micas (biotite, lepidolite, muscovite, and phlogopite) have K in the interlayer site between tetrahedral sheets. In other phyllosilicates (talc, serpentine), the interlayer site is absent or contains atoms other than K. The feldspars, a large and diverse group of minerals, are divided into two types: the K-feldspars ($(K,Na)AlSi_3O_8$) and plagioclase feldspar ($NaAlSi_3O_8$–$CaAl_2Si_2O_8$). Substitution of NaSi for CaAl in plagioclase is common, and practically any composition between the end-member compositions can crystallize on Earth. This study analyzed eight samples in the plagioclase solid solution series.

3. Experimental

3.1. Analytical methods

The ARL laboratory broadband LIBS system consists of a pulsed laser, mirror and focusing lens for laser light delivery, adjustable sample stage, a fiber optic for plasma light collection, broadband spectrometer, and desktop computer for system control and data collection. A 100 mJ laser pulse of 10 ns duration from an actively Q-switched Ultra Big Sky Technologies Nd–YAG laser operated at 1064 nm is focused by a

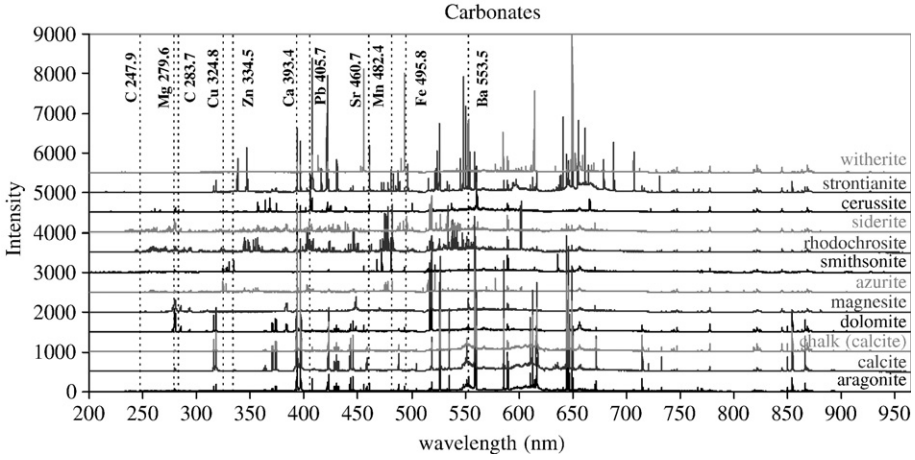

Fig. 2. Average LIBS spectra of representative carbonate minerals.

50 mm focal length convex lens to generate a high-temperature microplasma at the sample surface.

The sample to be analyzed was placed on a sample stage and the height adjusted manually so that the laser spark was observed to occur on the sample surface. The laser beam diameter was 3 mm, with a beam divergence of 1 mr, so that the laser spot size was about 60 μm and the crater generated on the sample was on the order of 100 μm diameter. A bundle of seven 600 μm core diameter optical fibers was oriented to collect the light emission from the plasma. The fibers transmitted the acquired light to an Ocean Optics, Inc., Model 2000 broadband spectrometer, having a resolution of 0.1 nm, to separate the light from different atomic, ionic, and molecular constituents of the plasma. The seven optical fibers were connected to seven separate spectrometers and gated CCD camera pairs; each pair covers one portion of the 198–964 nm spectral range. The LIBS spectra collection software and the statistical LIBS library software were provided by Ocean Optics Inc.

3.2. Data processing

Broadband LIBS spectra from 198 to 964 nm were collected from twenty laser shots for each of 52 minerals (18 carbonates, 9 pyroxenes and pyroxenoids, 6 amphiboles, 8 phyllosilicates, and 11 feldspars). Each laser shot was preceded with a cleaning shot, identical in energy with the subsequent analytical shot. The samples are natural minerals and chemically zoned on a scale of millimeters to centimeters. Thus, samples were moved several mm after each analytical shot to sample a new area on the mineral surface for the next analysis in order to capture a realistic average mineral composition. After the data collection, two composite spectra (averages of 10 shots each) were calculated for each sample to produce two databases each containing the composite LIBS spectra for the same 52 mineral samples.

The broadband LIBS spectra were compared to each other by calculating the correlation coefficient (R) of a linear correlation of the 13,605 pixel intensities from 198 to 964 nm for each pair of spectra (Fig. 1). Two very similar LIBS spectra would yield a correlation coefficient close to 1; The correlation coefficient decreases as the similarity between two spectra decreases. This method provides a simple and efficient way to compare many spectra and takes advantage of the totality of information contained in the broadband LIBS spectra.

4. Results and discussion

4.1. Carbonates

The carbonates yield highly variable LIBS spectra (Fig. 2), in part because of the high degree of ionic substitutions in both the rhombohedral and orthorhombic isostructural groups, with the chemical compositions of the different carbonate minerals clearly reflected in their spectra. For instance, smithsonite ($ZnCO_3$) is the only carbonate with Zn lines in its LIBS spectra (Fig. 2), the 405.8 nm Pb line is present for cerussite ($PbCO_3$), and witherite ($BaCO_3$) displays strong Ba lines. By contrast, Ca is an element that is widespread throughout the natural environment and, therefore, is present in most of the analyzed carbonates, except in the smithsonsites and magnesite ($MgCO_3$). Cu is present, as expected, in azurite ($Cu_3(CO_3)_2(OH)_2$) but is also detected in smithsonite. This is not surprising, because smithsonite occurs in weathered hydrothermal ore deposits, which commonly also are sources of both Cu and Zn.

The sensitivity of the LIBS spectra to carbonate chemistry suggests that it should be possible to discriminate between carbonate minerals using LIBS. This is demonstrated in Table 3, where the names and correlation coefficients for the five minerals with the most similar LIBS spectra are listed for the 52 minerals in this study. All 18 carbonate specimens were correctly identified, as defined by being the mineral with the highest correlation coefficient. Six samples (2 aragonites and 4 calcites) are polymorphs of $CaCO_3$. For most of these samples, each of the five best matches was a $CaCO_3$ polymorph (Table 3). The exception is calcite 2, which has pyroxenes (diopside — $CaMgSi_2O_6$, and augite — $(Ca,Na)(Mg,Fe,Al)(Si,Al)_2O_6$) and the carbonate dolomite — $CaMg(CO_3)_2$ as the most similar minerals. This sample is a black calcite, and correlates well to diopside, augite, and dolomite because of the presence of Ca, Mg, Fe, and relatively low Al. For similar reasons, dolomite correlates with calcite, diopside, and augite, and talc correlates with the magnesian silicate minerals talc and serpentine.

Some carbonate minerals do not match the spectra of other carbonates well. For instance, spectra of the three smithsonite samples (green, blue, and pink in color) correlate well to each other, despite the differences in color ($R=0.9381$–0.9945). However, the correlation coefficient for the next most similar sample is much lower (0.5670–0.6948), suggesting that it would be difficult to determine smithsonite's identity if a smithsonite spectra were not in the database. Similar relationships are observed for rhodochrosite ($MnCO_3$), cerussite ($PbCO_3$), strontianite ($SrCO_3$), witherite ($BaCO_3$), and azurite ($Cu_3(CO_3)_2(OH)_2$). The two averaged spectra for these minerals match well (and for the second rhodochrosite samples), but all other minerals only offer poor matches ($R<0.75$).

4.2. Pyroxenes and pyroxenoids

The pyroxenes and pyroxenoids are isostructural silicate mineral groups exhibiting a broad range of ionic substitution. The compositional differences are recorded in the LIBS spectra (Fig. 3), and all nine of these minerals were correctly identified (Table 3). The chemical associations observed in the carbonate data are seen in the pyroxene-pyroxenoid spectra as well. For instance, the Na–Fe pyroxene aegirine was found to be more similar to Na-rich feldspars than to the other pyroxenes, which tend to be Na-poor. Similarly, the LIBS spectra of the Li-rich pyroxene spodumene is similar to that of the Li-phyllosilicate lepidolite ($R=0.9050$), but not to any other mineral in our database ($R<0.75$).

4.3. Amphiboles

The amphibole isostructural group of silicate minerals is capable of incorporating an extremely wide variety of elements, as reflected in the LIBS spectra (Fig. 4). All six amphibole samples were correctly identified (Table 3). All of the analyzed

Table 3
Results of mineral identification experiment

Sample	Best match		Second best match		Third best match		Fourth best match		Fifth best match	
	Mineral	CC[a]	Mineral	CC	Mineral	CC	Mineral	CC	Mineral	CC
Carbonates										
Aragonite 1	Aragonite 1	0.9734	Calcite 3	0.9370	Calcite 4	0.9289	Calcite 1	0.9267	Aragonite 2	0.8716
Aragonite 2	Aragonite 2	0.9867	Calcite 3	0.9802	Calcite 4	0.9744	Calcite 1	0.9633	Aragonite 1	0.9219
Calcite 1	Calcite 1	0.9963	Calcite 3	0.9788	Aragonite 1	0.9710	Calcite 4	0.9237	Aragonite 2	0.9063
Calcite 2	Calcite 2	0.9933	Diopside 2	0.9482	Augite	0.9136	Diopside 1	0.9127	Dolomite	0.9091
Calcite 3	Calcite 3	0.9959	Calcite 1	0.9714	Aragonite 1	0.9483	Calcite 4	0.9429	Aragonite 2	0.9358
Calcite 4	Calcite 4	0.9914	Aragonite 2	0.9501	Calcite 3	0.9267	Calcite 1	0.9070	Aragonite 1	0.9007
Dolomite	Dolomite	0.9787	Diopside 2	0.9596	Calcite 2	0.9379	Diopside 1	0.9175	Augite	0.9108
Magnesite	Magnesite	0.9928	Talc	0.8817	Serpentine 2	0.8317	Siderite	0.7825	Orthopyroxene 1	0.7054
Rhodochrosite 1	Rhodochrosite 1	0.9916	Rhodochrosite 2	0.9652	Azurite	0.7043	Rhodonite	0.6684	Siderite	0.5050
Rhodochrosite 2	Rhodochrosite 2	0.9986	Rhodochrosite 1	0.9547	Azurite	0.6789	Rhodonite	0.6027	Siderite	0.4476
Siderite	Siderite	0.9890	Glaucophane	0.7907	Magnesite	0.7790	Actinolite	0.7634	Talc	0.7601
Smithsonite—blue	Smithsonite—blue	0.9945	Smithsonite—purple	0.9818	Smithsonite—green	0.9459	Plagioclase 5 (Ca–Na)	0.5670	Wollastonite	0.5669
Smithsonite—green	Smithsonite—green	0.9919	Smithsonite—purple	0.9481	Smithsonite—blue	0.9457	Plagioclase 1 (Na)	0.6948	K-feldspar 1	0.6877
Smithsonite—purple	Smithsonite—blue	0.9827	Smithsonite—purple	0.9791	Smithsonite—green	0.9381	Plagioclase 5 (Ca–Na)	0.6193	Wollastonite	0.6179
Cerussite	Cerussite	0.8941	K-feldspar 1	0.5474	K-feldspar 2	0.5350	Serpentine 1	0.5211	Plagioclase 1 (Na)	0.5184
Strontianite	Strontianite	0.9906	Cerussite	0.4246	Wollastonite	0.3954	Plagioclase 5 (Ca–Na)	0.3936	Tremolite	0.3838
Witherite	Witherite	0.9957	Cerussite	0.4336	Phlogopite	0.4182	Muscovite 1	0.2969	Smithsonite—green	0.2929
Azurite	Azurite	0.9881	Rhodonite	0.7413	Rhodochrosite 1	0.6537	Plagioclase 5 (Ca–Na)	0.6473	Rhodochrosite 2	0.6342
Pyroxenes and pyroxenoids										
Aegirine	Aegirine	0.9979	K-feldspar 3	0.9361	Plagioclase 4 (Na–Ca)	0.9289	Plagioclase 7 (Ca–Na)	0.9153	Plagioclase 1 (Na)	0.8998
Augite	Augite	0.9936	Diopside 1	0.9924	Wollastonite	0.9494	Diopside 2	0.9469	Calcite 2	0.9355
Diopside 1	Diopside 1	0.9969	Augite	0.9944	Wollastonite	0.9448	Actinolite	0.9239	Diopside 2	0.9222
Diopside 2	Diopside 2	0.9972	Calcite 2	0.9343	Dolomite	0.9342	Diopside 1	0.9180	Augite	0.9116
Orthopyroxene 1	Orthopyroxene 1	0.9896	Orthopyroxene 2	0.9870	Serpentine 1	0.9547	Anthophyllite	0.9255	Serpentine 2	0.9001
Orthopyroxene 2	Orthopyroxene 2	0.9912	Orthopyroxene 1	0.9741	Anthophyllite	0.9582	Serpentine 1	0.9387	Tremolite	0.9054
Rhodonite	Rhodonite	0.9947	Plagioclase 8 (Ca–Na)	0.8965	Plagioclase 5 (Ca–Na)	0.8911	Tremolite	0.8878	Glaucophane	0.8619
Spodumene	Spodumene	0.9733	Lepidolite	0.9050	Anthophyllite	0.7404	Hornblende	0.7365	Muscovite 2	0.6869
Wollastonite	Wollastonite	0.9957	Diopside 1	0.9540	Augite	0.9506	Diopside 2	0.9323	Plagioclase 5 (Ca–Na)	0.9285

Amphiboles										
Actinolite	Actinolite	0.9834	Glaucophane	0.9626	Tremolite	0.9506	Augite	0.9185	Diopside 1	0.9141
Anthophyllite	Anthophyllite	0.9829	Glaucophane	0.9183	Tremolite	0.9160	Hornblende	0.9061	Orthopyroxene 2	0.8839
Glaucophane	Glaucophane	0.9840	Tremolite	0.9528	Anthophyllite	0.9449	Actinolite	0.9320	Orthopyroxene 2	0.9023
Hornblende	Hornblende	0.9788	Aegirine	0.9309	Plagioclase 7 (Ca–Na)	0.9055	K-feldspar 3	0.9048	Plagioclase 2 (Na)	0.8746
Riebeckite	Riebeckite	0.9981	Plagioclase 7 (Ca–Na)	0.8925	Aegirine	0.8337	K-feldspar 3	0.8047	Hornblende	0.7374
Tremolite	Tremolite	0.9850	Plagioclase 6 (Ca–Na)	0.9516	Plagioclase 8 (Ca–Na)	0.9445	Glaucophane	0.9288	Plagioclase 5 (Ca–Na)	0.9265
Phyllosilicates										
Biotite	Biotite	0.9703	Phlogopite	0.9336	Anthophyllite	0.8625	Muscovite 1	0.8624	Orthopyroxene 1	0.8326
Muscovite 1	Muscovite 1	0.9904	Muscovite 2	0.8834	Hornblende	0.8800	K-feldspar 3	0.8437	Anthophyllite	0.8304
Muscovite 2	Muscovite 2	0.9809	K-feldspar 1	0.9581	K-feldspar 2	0.9387	Anthophyllite	0.8933	Serpentine 1	0.8726
Lepidolite	Lepidolite	0.9758	K-feldspar 1	0.8801	Muscovite 2	0.8755	Anthophyllite	0.8631	K-feldspar 2	0.8594
Phlogopite	Phlogopite	0.9952	Biotite	0.9233	Serpentine 2	0.8513	Talc	0.8349	Anthophyllite	0.8144
Serpentine 1	Serpentine 1	0.9951	Orthopyroxene 1	0.9545	Orthopyroxene 2	0.9514	K-feldspar 2	0.9272	Anthophyllite	0.9012
Serpentine 2	Serpentine 2	0.9970	Talc	0.9441	Orthopyroxene 1	0.9049	Orthopyroxene 2	0.8819	Phlogopite	0.8686
Talc	Talc	0.9829	Serpentine 2	0.9115	Magnesite	0.8552	Phlogopite	0.7937	Orthopyroxene 1	0.7541
Feldspars										
K-feldspar 1	K-feldspar 1	0.9888	K-feldspar 2	0.9766	Muscovite 2	0.9300	Plagioclase 1 (Na)	0.9296	Plagioclase 4 (Na–Ca)	0.9243
K-feldspar 2	K-feldspar 2	0.9903	K-feldspar 1	0.9681	Muscovite 2	0.9406	Plagioclase 1 (Na)	0.9055	Serpentine 1	0.9049
K-feldspar 3	K-feldspar 3	0.9813	Plagioclase 7 (Ca–Na)	0.9455	Aegirine	0.9421	Plagioclase 4 (Na–Ca)	0.8784	Riebeckite	0.8578
Plagioclase 1 (Na)	Plagioclase 1 (Na)	0.9723	Plagioclase 4 (Na–Ca)	0.9642	Aegirine	0.9637	Plagioclase 6 (Ca–Na)	0.9416	Plagioclase 2 (Na)	0.9336
Plagioclase 2 (Na)	Plagioclase 2 (Na)	0.9942	Aegirine	0.9327	Plagioclase 1 (Na)	0.8908	Plagioclase 6 (Ca–Na)	0.8874	Plagioclase 3 (Na–Ca)	0.8858
plagioclase 3 (Na–Ca)	plagioclase 3 (Na–Ca)	0.9958	plagioclase 6 (Ca–Na)	0.9675	plagioclase 5 (Ca–Na)	0.9537	plagioclase 8 (Ca–Na)	0.9534	plagioclase 1 (Na)	0.9472
plagioclase 4 (Na–Ca)	plagioclase 4 (Na–Ca)	0.9829	plagioclase 1 (Na)	0.9787	K-feldspar 1	0.9381	plagioclase 6 (Ca–Na)	0.9325	K-feldspar 3	0.9129
Plagioclase 5 (Ca–Na)	Plagioclase 5 (Ca–Na)	0.9909	Plagioclase 8 (Ca–Na)	0.9872	Plagioclase 3 (Na–Ca)	0.9660	Plagioclase 6 (Ca–Na)	0.9523	Tremolite	0.9346
Plagioclase 6 (Ca–Na)	Plagioclase 6 (Ca–Na)	0.9854	Plagioclase 1 (Na)	0.9725	Plagioclase 3 (Na–Ca)	0.9501	Plagioclase 8 (Ca–Na)	0.9397	Plagioclase 4 (Na–Ca)	0.9304
Plagioclase 7 (Ca–Na)	Plagioclase 7 (Ca–Na)	0.9990	Aegirine	0.9265	K-feldspar 3	0.8962	Riebeckite	0.8917	Plagioclase 2 (Na)	0.8650
Plagioclase 8 (Ca–Na)	Plagioclase 8 (Ca–Na)	0.9694	Plagioclase 6 (Ca–Na)	0.9514	Plagioclase 3 (Na–Ca)	0.9451	Plagioclase 2 (Na)	0.9408	Plagioclase 5 (Ca–Na)	0.9334

[a] Correlation coefficient.

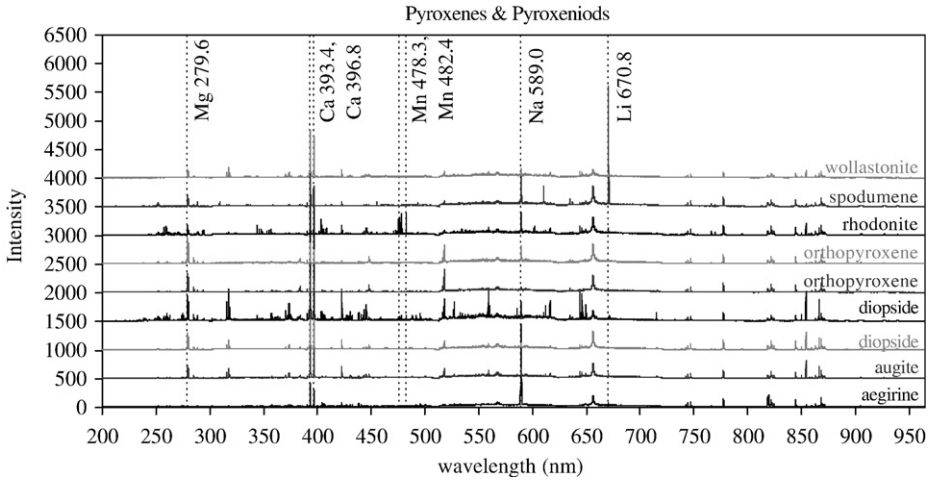

Fig. 3. Average LIBS spectra of representative pyroxenes and pyroxenoids.

samples are rich in Mg, except riebeckite ($Na_2Fe_5Si_8O_{22}(OH)_2$), which is clearly seen in the intensity of the Mg 279.6 nm line (Fig. 4) as well as in the similarity between riebeckite and the Na-feldspars rather than the other amphiboles (Table 3). The five most similar spectra for the amphiboles were from other amphiboles (42%), from the closely compositionally related pyroxenes (25%), and from the feldspars (33%), suggesting that this method of comparing broadband LIBS spectra is most sensitive to mineral elemental composition rather than stoichiometry. For instance, hornblende ($(Ca,Na)_{2-3}(Mg,Fe,Al)_5Si_6(Si,Al)_2O_{22}(OH)_2$) can be considered to be actinolite ($Ca_2(Mg,Fe)_5Si_8O_{22}(OH)_2$) with the addition of Al and Na. However, the composition of hornblende analyzed in this study is more similar to aegirine ($NaFeSi_2O_6$) and the feldspars ($R=0.8746–0.9309$) than to actinolite, $Ca_2(Mg,Fe)_5Si_8O_{22}(OH)_2$ ($R=0.6477$). An unexpected result of LIBS analysis of amphiboles is the ubiquitous presence of Li (Fig. 4), even in amphiboles that crystallized in geologic environments that are expected to be Li-poor (anthophyllite in metamorphosed ultramafic metamorphic rocks, for example). The sensitivity of LIBS to Li has great promise for the quantitative analysis of Li in Earth minerals [9] as well as for discriminating between various rock types on Mars (Wiens, personal communication, 2006).

4.4. Phyllosilicates

Two types of phyllosilicates were analyzed in this study: the micas with K^+ in the interlayer site between the layers of tetrahedral and octahedral sheets (biotite, muscovite, phlogopite, and lepidolite), and those minerals with a vacant or missing interlayer site (serpentine, talc). These differences are seen in the LIBS data; all eight samples were correctly identified (Table 3). The presence of K^+ in the mica interlayer site is clearly seen in the LIBS spectra (Fig. 5). The Mg-rich nature of talc, serpentine, phlogopite, and biotite is reflected in the LIBS spectra for these minerals, as is the Mg-poor nature of muscovite and lepidolite. As observed in the amphibole data, Li is nearly ubiquitous, present even in talc and one serpentine sample, which crystallize

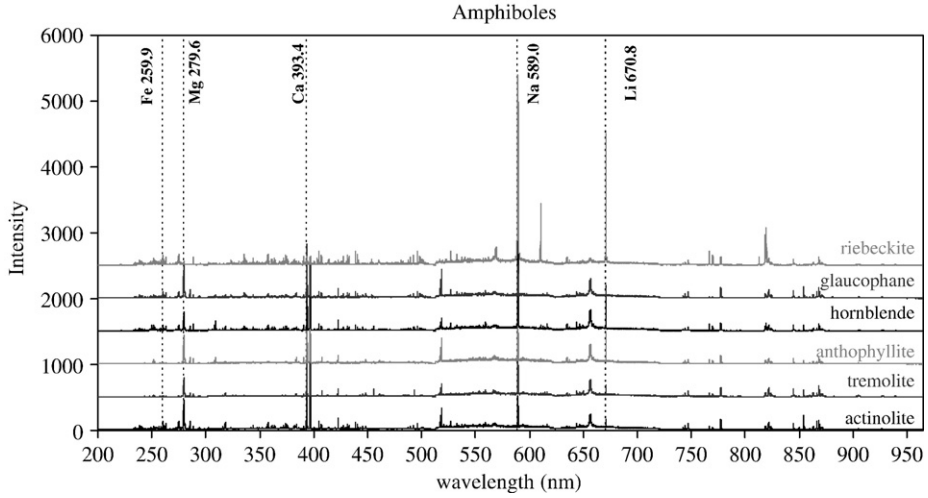

Fig. 4. Average LIBS spectra of representative amphiboles.

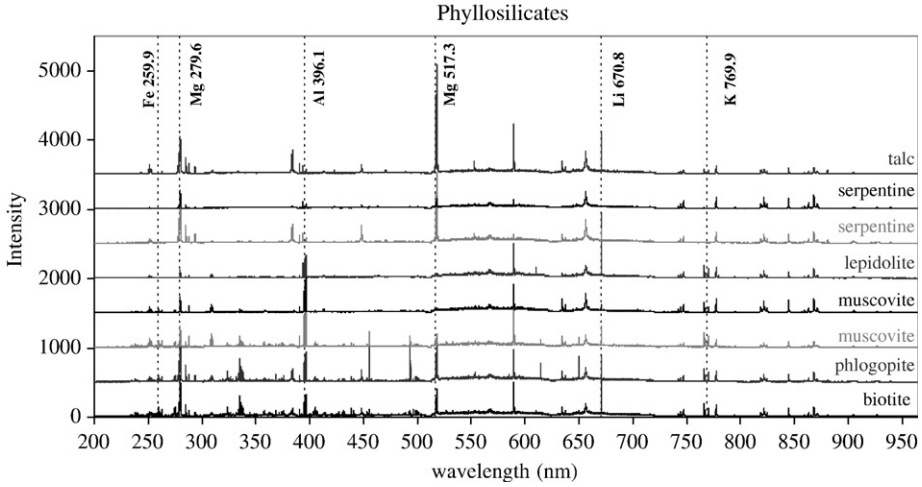

Fig. 5. Average LIBS spectra of representative phyllosilicates.

in ultramafic metamorphic rocks that are widely regarded to contain little Li.

4.5. Feldspars

The feldspars crystallize across the entire range of temperatures and pressures realized in igneous, metamorphic and sedimentary rocks and therefore comprise much of the Earth's crust. The structure of these minerals allows significant ionic substitution that records details of the changing geochemical environment of their formation. Thus, the ability to quickly distinguish large numbers of feldspar samples on the basis of their chemical compositions would enhance the understanding of large bodies of rocks such as metamorphic belts and plutons and be very helpful in economic mineral exploration. Representative feldspar LIBS spectra are presented in Fig. 6; all feldspar samples were correctly identified (Table 3). The chemistry of the feldspars is expressed in the observed LIBS spectra; K-feldspar is the only sample containing a significant K peak and the Na peak intensity is lower for the calcic plagioclase samples than for the sodic plagioclase samples.

4.6. Mineral identification using LIBS

Although it is encouraging that all of the samples in this study were correctly identified by comparing two averaged LIBS spectra, an important related experiment can be realized by examining the second most similar spectra in Table 3. This simulates the case in which a potentially similar mineral, although not the same sample, exists in the data set. In this case, the existing data set of 52 minerals is insufficient to portray the variety of mineral compositions observed on Earth. However, the exercise reveals interesting aspects of LIBS systematics.

Using only the second best matched minerals listed in Table 3, 65% (34 of 52) of the minerals were identified as a mineral from the same mineral family (carbonate, pyroxene/pyroxenoid, amphibole, phyllosilicate, or feldspar). This percent changes slightly from family to family, from 50% of the amphiboles to 82% of the feldspars, depending on the overall compositional variability present in the family. There were two reasons that minerals were misidentified as a mineral of a different family. The first reason is that the mineral contains a dominant element that is not present in

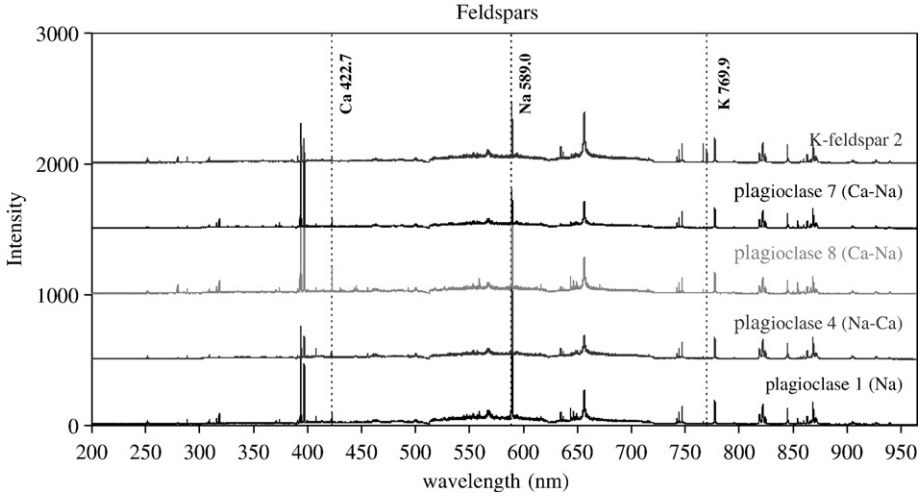

Fig. 6. Average LIBS spectra of representative feldspars.

the other minerals in the data base. These matches have low correlation coefficients (<0.80); examples are the carbonates cerussite ($PbCO_3$), azurite ($Cu_3(CO_3)_2(OH)_2$), and siderite ($FeCO_3$). Smithsonite ($ZnCO_3$) shows the same behavior; the correlation coefficients for other smithsonite samples are high (R=0.9381–0.9818), but the next most similar spectra have low correlation coefficients (R<0.70). Identification of these minerals would not be possible without having a representative sample in the database.

Other minerals that were misidentified by the second match have relatively high correlation coefficients (R>0.85). These minerals' spectra were matched to minerals with similar elemental composition but different stoichiometry. For instance, two Ca–Mg carbonates (calcite 2 and dolomite) were matched to the Ca–Mg silicate diopside, $CaMgSi_2O_6$, and the Mg carbonate magnesite ($MgCO_3$) was matched to the Mg silicate talc ($Mg_3Si_4O_{10}(OH)_2$). There was a high correlation between non-silicate carbonate and silicate spectra because even the major Si (288.16 nm) and C (247.9, 283.7 nm) peaks have low intensity in minerals (Fig. 2). Similarly, the phyllosilicates muscovite 2, lepidolite, and serpentine 1 were matched to other silicates with similar elemental composition (K-feldspar 1, K-feldspar 1, and orthopyroxene, respectively). The match between the Li mica lepidolite, $(K(Li,Al)_{2-3}AlSi_3O_{10}(O,OH,F)_2)$, and K-feldspar 1, $((K,Na)AlSi_3O_8)$, occurs because of the K and Al peaks. Serpentine, $Mg_6Si_4O_{10}(OH)_8$, and orthopyroxene, $(Mg,Fe)SiO_3$, are similar Mg-rich, Ca-poor silicates. The two feldspar samples that were misidentified by their second matches were both matched to the Na pyroxene aegirine, ($NaFeSi_2O_6$), because of the intense Na peaks. These relationships suggest that mineral identification by LIBS is driven by elemental composition, as would be expected. Because a mineral may be misidentified as a member of a different mineral family, it is important to recognize that LIBS is yielding compositional, and not stoichiometric information.

5. Conclusions

This study demonstrates that broadband LIBS spectra can be used to correctly identify minerals from the carbonate and silicate families. By comparing averaged LIBS spectra against a library of the same mineral spectra, 100% of the 52 minerals in the database were correctly identified. If a mineral's spectrum was compared to the other 51 minerals, there was a 65% chance that it would be identified as a mineral of the same family (carbonate, pyroxene/pyroxenoid, amphibole, phyllosilicate, or feldspar). However, all minerals were correctly identified by their dominant elements (Mg-rich minerals, Ca-rich minerals, etc.), except for those with an element that did not exist in any other mineral in the database. This study provides support for the continued development of LIBS, especially portable LIBS, for applications in the geological sciences.

Acknowledgements

The first author gratefully acknowledges Hispanic-serving Institution Grant award # W911NF-06-1-0005 from the Army Research Office.

References

[1] C. Klein, B. Dutrow, Mineral Science, 23rd ed., John Wiley & Sons, New York, 2008.
[2] P.J. Potts, A Handbook of Silicate Rock Analysis, Blackie & Son Limited, Glasgow, 1987.
[3] R.T. Wainner, R.S. Harmon, A.W. Miziolek, K.L. McNesby, P.D. French, Analysis of environmental lead contamination: comparison of LIBS field and laboratory instruments, Spectrochim. Acta Part B 56 (2001) 777–793.
[4] R.S. Harmon, F.C. De Lucia, A.W. Miziolek, K.L. McNesby, R.A. Walters, P.D. French, Laser-induced breakdown spectroscopy (LIBS) — an emerging field-portable sensor technology for real-time, in-situ geochemical and environmental analysis, Geochem., Explor. Environ. Anal. 5 (2005) 21–28.
[5] B. Salle, J.L. Lacour, E. Vors, P. Fichet, S. Maurice, D.A. Cremers, R.C. Weins, Laser Induced Breakdown Spectroscopy for Mars surface analysis: capabilities and standoff distances, and detection of sulfur and chlorine elements, Spectrochim. Acta Part B 59 (2002) 1413–1422.
[6] J.J. Gurney, A comparison between garnet and diamonds in kimberlites, in: J.E. Glover, P.G. Harris (Eds.), Kimberlite Occurrence and Origin: A Basis of Conceptual Models in Exploration, University of Western Australia, Perth, 1984, Publication B.
[7] J.J. Gurney, P. Zweistra, The interpretation of the major element compositions of mantle minerals in diamond exploration, in: W.L. Griffin (Ed.), Diamond exploration into the 21st century, J. Geochem. Explor., 53, 1995, pp. 293–309.
[8] R.J. Parker, K. Nicholson, As in geothermal sinters: determination and implications for mineral exploration, in: C.C. Harvey, P.R.L. Broen, D.H. Freestone, G.L. Scott (Eds.), Proceedings of the 12th New Zealand Geothermal Workshop, Auckland University Press, 1990, pp. 35–39.
[9] C. Fabre, M.C. Boiron, J. Dubessy, A. Chabiron, B. Charov, T.M. Crespo, Advances in lithium analysis in solids by means of laser-induced breakdown spectroscopy: an exploratory study, Geochim. Cosmochim. Acta 66 (2002) 1401–1407.